Magnetic Resonance Imaging 57 (2019) 68–74

Contents lists available at ScienceDirect

Magnetic Resonance Imaging

journal homepage: www.elsevier.com/locate/mri

Original contribution

Associations between whole tumor histogram analysis parameters derived from ADC maps and expression of EGFR, VEGF, Hif 1-alpha, Her-2 and Histone 3 in uterine cervical cancer

Hans-Jonas Meyer[a,*,1], Peter Gundermann[a,1], Anne Kathrin Höhn[b], Gordian Hamerla[a], Alexey Surov[a]

[a] Department of Diagnostic and Interventional Radiology, University of Leipzig, Liebigstraße 20, D-04103 Leipzig, Germany
[b] Department of Pathology, University of Leipzig, Liebigstraße 20, D-04103 Leipzig, Germany

ARTICLE INFO

Keywords:
Cervical cancer
Magnetic resonance imaging
Diffusion weighted imaging

ABSTRACT

Objective: Diffusion weighted imaging (DWI) can be quantified by apparent diffusion coefficient (ADC) and can predict tissue microstructure. The aim of the present study was to analyze possible associations between ADC histogram based parameters with different histopathological parameters in cervical squamous cell carcinoma.
Materials and methods: 18 female patients (age range 32–79 years) with squamous cell cervical carcinoma were retrospectively enrolled. In all cases, pelvic MRI was performed with a DWI (b-values 0 and 1000 s/mm^2). Histogram analysis was performed as a whole lesion measurement. Histopathological parameters included expression of EGFR, VEGF, Hif1-alpha, Her2 and Histone 3. Spearman's correlation coefficient was used to analyze associations between investigated parameters.
Results: Analyze of the investigated ADC histogram parameters showed a good interreader variability, ranging from 0.705 for entropy to 0.959 for ADCmedian. EGFR expression correlated statistically significant with several histogram parameters. The highest correlation was observed for p75 ($p = -0.562$, $P = 0.015$). There were several correlations with histone 3, the highest with p25 ($p = -0.610$, $P = 0.007$). None of the ADC related parameters correlated statistically significant with expression of VEGF, Hif1-alpha and Her2.
Conclusion: Histogram analysis showed a good interreader agreement. ADC histogram parameters might be able to reflect expression of EGFR and histone 3 in cervical squamous cell carcinomas, but not expression of VEGF, Hif1-alpha and Her2.

1. Introduction

Cervical cancer is the third most commonly diagnosed cancer and the fourth leading cause of cancer death in females worldwide [1].

Magnetic resonance imaging (MRI) has been established as the best imaging modality for staging of cervical cancers due to its excellent soft tissue contrast [2]. Furthermore, MRI can provide information regarding tumor microstructure by using diffusion-weighted imaging (DWI). The principal hypothesis is that DWI can quantify free movement of water molecules (Brownian molecular movement) by means of apparent diffusion coefficients (ADC) [3]. In tissues, this movement is hindered predominantly by cells. Previously, numerous reports observed inverse correlations between ADC and cellularity in several malignant and benign lesions [4]. Moreover, malignant tumors showing significant lower ADC values than benign tumors [3].

Also in cervical cancer, it has been shown that ADC inversely correlated with cellularity [5,6]. Moreover, a statistically significant correlation between ADC and proliferation index Ki67 could be identified [7]. These data indicated that ADC values can be used as imaging biomarker.

An emergent imaging analysis, namely histogram analysis, can be further used for more thorough tumor investigations. This method includes an analysis of every voxel in a region of interest. This results in a histogram distribution of acquired parameters [8]. Typically histogram parameters are percentiles, median, mode, skewness, kurtosis and entropy. As reported previously, heterogeneity displayed by the histogram

* Corresponding author.
E-mail addresses: Hans-jonas.meyer@medizin.uni-leipzig.de (H.-J. Meyer), peter.gundermann@medizin.uni-leipzig.de (P. Gundermann), annekathrin.hoehn@medizin.uni-leipzig.de (A.K. Höhn), Gordian.hamerla@medizin.uni-leipzig.de (G. Hamerla), alexey.surov@medizin.uni-leipzig.de (A. Surov).
[1] These authors contributed equally.

https://doi.org/10.1016/j.mri.2018.10.016
Received 9 August 2018; Received in revised form 23 September 2018; Accepted 22 October 2018

might reflect heterogeneity of tumor microstructure [8]. Therefore, a better prediction of tumor biology by imaging may be possible [8]. There were only few studies about ADC histogram analysis in cervical cancer [9–14]. For instance, it has been shown that all derived histogram parameters can discriminate between cervical physiological tissue and cancer [11]. Additionally, one study identified a statistically significant correlation between entropy and p53 positive cells [9]. Finally, histogram analysis was superior in prediction of tumor recurrence than conventional region-of-interest-based ADC analysis [10].

According to the literature, several histopathological features are clinically important in cervical cancer [15–17]. There include expression of epidermal-growth factor (EGFR), hypoxia-inducible factor 1-alpha (Hif1-alpha), vascular endothelial growth factor (VEGF), human epidermal growth factor receptor 2 (Her2) and Histone 3, which are related to prognosis and prediction of treatment success [15–17]. Presumably, histogram based ADC parameters might be able to predict some of these histolopathological features in cervical cancer.

Therefore, the aim of this study was to elucidate possible associations between ADC histogram based parameters and expression of EGFR, Hif1-alpha, VEGF, Her2 receptor and Histone 3 in cervical cancer.

2. Patients and methods

This retrospective study was approved by the local research ethics committee.

2.1. Patients

The patient sample of the present study comprised 18 female patients (age range 32–79 years; mean age 55.4 years) with squamous cell cervical carcinoma. Table 1 summarizes the characteristics of the patient sample. All patients were investigated before any form of treatment.

2.2. MRI

In all cases, pelvic MRI was performed. Our investigation protocol included the following sequences: an axial T2 weighted (T2w) turbo spin echo (TSE) sequence (TR/TE: 5590/105), a sagittal T2w TSE sequence (TR/TE: 4110/131), an axial T1 weighted (T1w) TSE sequence (TR/TE:1310/12), an axial T1 TSE sequence after intravenous application of contrast medium (0.1 mmol/kg body weight Gadobutrol, Bayer Healthcare, Germany) (TR/TE:912/12), and a sagittal post contrast T1 TSE (TR/TE: 593/12). DWI was performed using a multi-shot SE-EPI sequence (EPI) sequence (b 0 and b 1000 s/mm^2, repetition time: 4900 ms; echo time: 105 ms; slice thickness: 5 mm; matrix: 88 × 134; field of view: 450 × 450 mm). Fig. 1 shows an exemplary patient of our patient sample.

Table 1
Clinical data of the investigated patients and tumors.

Case	Age	Tumor grade	T stage	N stage	M stage
1	63	G2	2b	1	0
2	76	G3	4	0	0
3	65	G2	2b	0	0
4	63	G3	4	1	1
5	34	G3	2b	1	0
6	57	G2	4	1	1
7	53	G3	2b	0	0
8	32	G2	4	1	0
9	32	G2	2b	0	0
10	54	G2	3a	2	0
11	79	G3	4	1	0
12	52	G1	4	0	0
13	37	G3	2b	1	1
14	72	G3	4	0	0
15	46	G2	2b	1	1
16	71	G2	4	1	1
17	50	G2	2b	1	1
18	61	G2	4	1	0

2.3. Histogram analysis of ADC values

Automatically generated ADC maps were transferred in DICOM format and processed offline with custom-made Matlab-based application (The Mathworks, Natick, MA). The ADC maps were displayed within a graphical user interface (GUI), which enables the reader to scroll through the slices and draw a volume of interest (VOI) at the

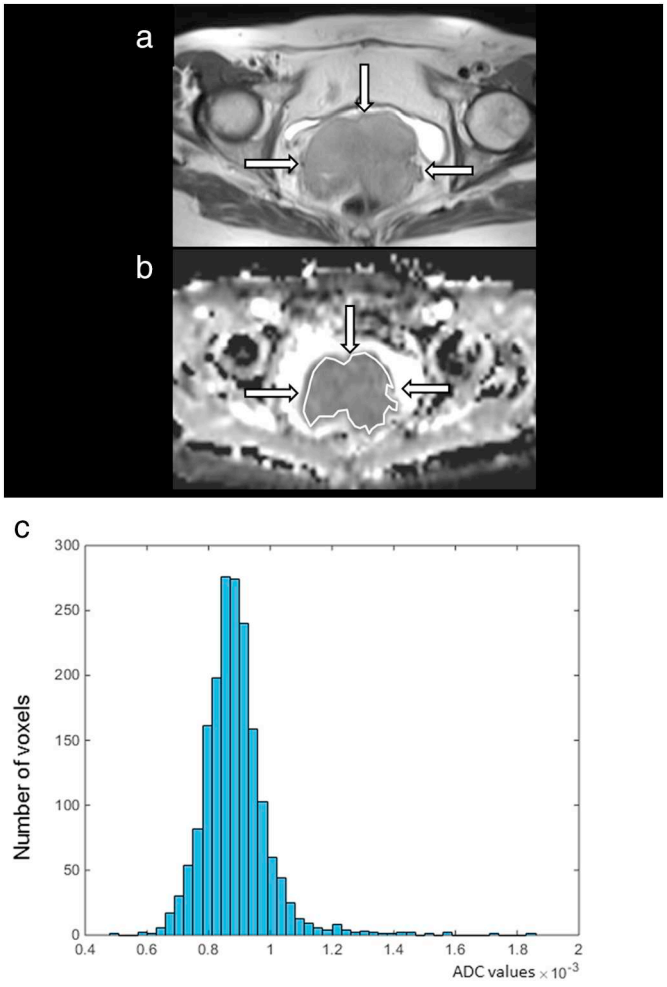

Fig. 1. Imaging and histopathological findings in a patient with T4a N0 M0 uterine cervical cancer.
a. T2-weighted TSE image showing a large lesion in the uterine cervix (arrows).
b. ADC map of the tumor with a ROI.
c. Histogram of ADC values. Histogram analysis parameters ($\times 10^{-3}$ mm^2/s) of the lesion are as follows: ADCmean = 0.89, ADCmin = 0.49, ADCmax = 1.86, p10 = 0.78, p25 = 0.83, p75 = 0.93, p90 = 1.0, median = 0.88, mode = 0.87. Furthermore, statistical histogram parameters are as follows: kurtosis = 13.79, skewness = 1.93, entropy = 3.67.
d. EGFR staining and particle tool analysis image. Stained area is 5.3%.
e. Her-2 stained specimen and particle tool analysis image. There were no positive stained cells.
f. Hi1-alpha stained specimen and particle tool analysis image. Stained area is 28.9%.
g. Histone 3 stained specimen and particle tool analysis image. Stained area is 22.3%.
h. VEGF stained specimen and particle tool analysis image. Stained area is 57.8%.

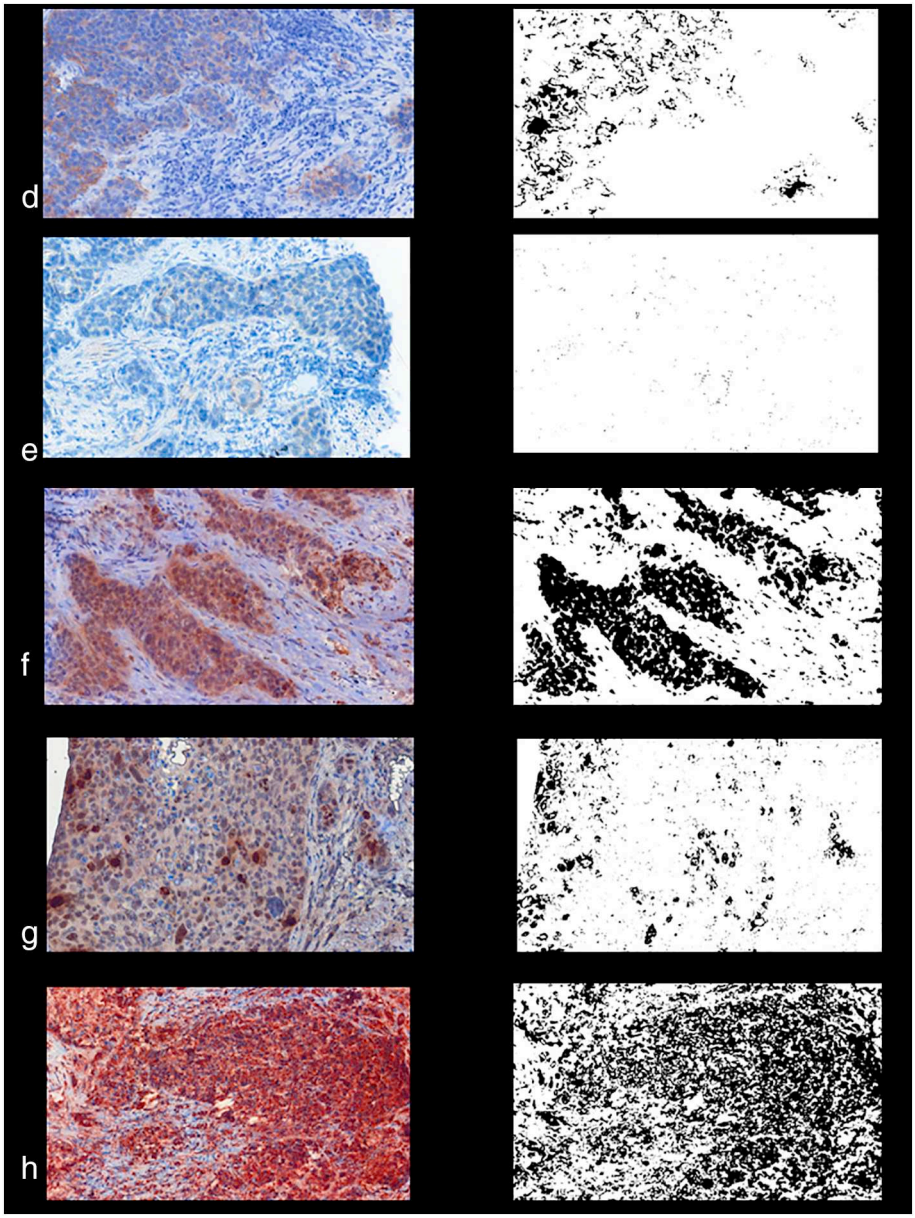

Fig. 1. (*continued*)

tumor's boundary, in accordance to the T2-weighted and images (whole lesion measure). All measures were performed by two authors independently to each other and blinded to histopathology (AS with 15 years and HJM with 2 years of radiological experience, respectively). The ROIs were modified in the GUI and saved (in Matlab-specific format) for later processing. Following parameters were calculated: mean (ADC_{mean}), maximum (ADC_{max}), minimum (ADC_{min}), median, 10th (p10 ADC), 25th (p25 ADC), 75th (p75 ADC), 90th (p90 ADC) percentile, and mode (ADC mode). Additionally, histogram-based characteristics of the ROI - kurtosis, skewness and entropy – were calculated according to our previous description [9].

2.4. Histopathological analysis

In all cases the diagnosis was confirmed histopathologically by tumor biopsy. All histopathological specimens were analyzed by a board specified pathologist with 11 years of experience (AKH). The biopsy specimens were deparaffinized, rehydrated and cut into 5 µm slices. Thereafter, the histological slices were stained by epidermal growth factor receptor (EGFR, EMERGO Europe, clone 111.6, dilution 1:30), vascular endothelial growth factor (VEGF, EMERGO Europe, clone VG1, dilution 1:20), hypoxia-inducible factor (HIF-1α Biocare Medical, 60 Berry Dr. Pacheco, CA 94553; clone EP1215Y, dilution 1:100), Histone 3 (Phospho- Histone H3, Biocare Medical; polyclone rabbit antibody, dilution 1:100), Human epidermal growth factor receptor-2 (Her2, clone 4B5, Roche Diagnostics, 6 mkg/ml).

On the next step, all stained specimens were digitalized by using the Pannoramic microscope scanner (Pannoramic SCAN, 3DHISTECH Ltd., Budapest, Hungary) with Carl Zeiss objectives up to 41× bright field magnification by default. Furthermore, the slides were evaluated via Pannoramic Viewer 1.15.4 (open source software, 3D HISTECH Ltd., Budapest, Hungary) and three captures with a magnification of x200 were extracted of each sample.

The histopathological images were further analyzed by using the ImageJ software 1.48v (National Institutes of Health Image program).

For quantification of the staining, a threshold was set for the RGB image (uncompressed.tif) using the Image-Adjust-Color Threshold tool. The intensity control was adjusted so that the threshold mask matched the staining coloring. This was performed semiautomatically with manual correction by one author (HJM) (Fig. 1d–h). Finally, expression

Table 2
Mean ± SD of the investigated parameters in the whole patient sample.

Parameters	Mean ± SD	Range
Mean, $\times 10^{-3}$ mm²/s	0.96 ± 0.14	0.71–1.16
Min, $\times 10^{-3}$ mm²/s	0.51 ± 0.20	0.26–0.83
Max, $\times 10^{-3}$ mm²/s	1.71 ± 0.29	1.10–2.44
P10, $\times 10^{-3}$ mm²/s	0.70 ± 0.14	0.51–0.90
P25, $\times 10^{-3}$ mm²/s	0.83 ± 0.13	0.66–1.07
P75, $\times 10^{-3}$ mm²/s	1.10 ± 0.23	0.79–1.75
P90, $\times 10^{-3}$ mm²/s	1.34 ± 0.28	0.90–1.96
Median, $\times 10^{-3}$ mm²/s	0.92 ± 0.13	0.68–1.16
Mode, $\times 10^{-3}$ mm²/s	0.91 ± 0.12	0.69–1.15
Kurtosis	4.62 ± 1.99	2.40–10.10
Skewness	0.77 ± 0.82	−0.80-2.10
Entropy	3.54 ± 0.93	1.88–5.14
EGFR, %	26.9 ± 22.58	0–72
Her 2, %	7.86 ± 18.32	0–64
Hif1-alpha, %	29.78 ± 21.81	5.10–84.57
Histone 3, %	26.84 ± 23.25	0.61–81.65
VEGF, %	28.04 ± 21.04	0.65–61.14

of EGFR, VEGF, and HIF-1α were estimated as a percent of stained areas per high power field according to previous description [9,16].

The tumors were divided according to the Her2-status in Her2-positive and Her2-negative.

2.5. Statistical analysis

Statistical analysis was performed using SPSS 23.0 (SPSS Inc., Chicago, IL). Collected data were evaluated by means of descriptive statistics. Spearman's correlation coefficient (ρ) was used to analyze associations between investigated parameters. Inter-reader variability was assessed with intraclass coefficients. P-values < 0.05 were taken to indicate statistical significance.

3. Results

The descriptive details including mean values and standard deviation of the analyzed parameters are summarized in Table 2.

The investigated ADC histogram parameters showed a good inter-reader variability, ranging from ICC = 0.705 for entropy to ICC = 0.959 for ADCmedian (Table 3).

Spearman's correlation analysis identified several statistically significant correlations between ADC histogram parameters and EGFR expression (Fig. 2). The best correlation was found for p75 ($\rho = -0.562$, P = 0.015) (Table 4). Moreover, several ADC histogram analysis parameters correlated significantly with expression of histone 3 (Table 4, Fig. 3). No statistically significant correlations were observed between ADC histogram analysis parameters and expression of VEGF and/or Hif1-alpha (Fig. 4). There were also no statistically significant differences of ADC related parameters between Her2-positive and Her2-negative tumors (Table 5).

Table 3
Interreader variability with intraclass coefficients of the investigated ADC parameters.

ADC parameters	ICC
Mean, $\times 10^{-3}$ mm²/s	0.870
Min, $\times 10^{-3}$ mm²/s	0.947
Max, $\times 10^{-3}$ mm²/s	0.920
P10, $\times 10^{-3}$ mm²/s	0.727
P25, $\times 10^{-3}$ mm²/s	0.844
P75, $\times 10^{-3}$ mm²/s	0.804
P90, $\times 10^{-3}$ mm²/s	0.803
Median, $\times 10^{-3}$ mm²/s	0.959
Mode, $\times 10^{-3}$ mm²/s	0.917
Kurtosis	0.859
Skewness	0.792
Entropy	0.705

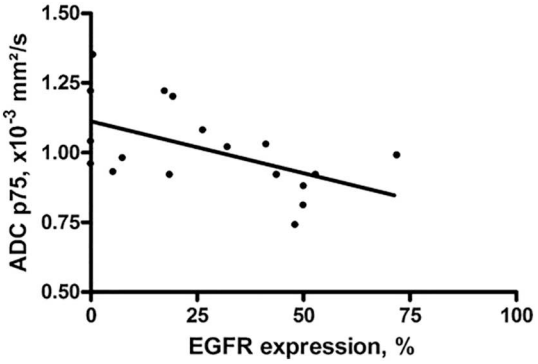

Fig. 2. Correlation graph between ADCp75 and EGFR expression. The Spearman correlation coefficient is $\rho = -0.562$ (P = 0.015).

4. Discussion

The present study identified associations between different histopathological features and ADC histogram based parameters in cervical cancer.

Previously, the possible benefit of DWI in cervical cancer diagnostics has been widely acknowledged [5–7,9–14]. For example, DWI can differentiate between tumor tissue and physiological uterine cervix tissue [11]. Furthermore, DWI can predict prognosis and treatment response for radiotherapy [18]. Additionally, it can also provide information regarding tumor microstructure [7,19].

Numerous studies showed associations between ADC values and cell density in several tumors [4]. Also in cervical cancer, different ADC parameters correlated with cellularity [4–6]. However, there is increasing evidence that ADC values might also be associated with further tumor characteristics like proliferation index or microvessel density [20,21]. ADC values might be able to predict non-invasively relevant information regarding tumor composition and receptor status.

As mentioned above, recently, a novel imaging approach has been established, namely histogram analysis [8]. In cervical cancer, histogram analysis derived from ADC maps has been investigated in several studies [9–14]. So far, skewness can distinguish adenocarcinomas from squamous cell carcinomas [13]. Moreover, as reported previously, some histogram based parameters might be different between tumor grades. [9,13,14]. For instance, it has been shown that histogram analysis based parameters of pseudodiffusion D* can differentiate between early and advanced stage cervical cancer [23]. Furthermore, the 5th percentile ADC was reported as the best histogram parameter for distinguishing well/moderately tumors from poorly differentiated squamous cell carcinomas [24]. Moreover, according to the literature, histogram analysis could also predict treatment response [10,12]. So far, ADC mode, 5th, 10th, and 25th percentiles changed significantly under chemotherapy, which might aid in tumor follow up investigations [22]. Additionally, it has been reported that the shape of the histogram significantly changed during radiotherapy. The shape leans toward the right end and turned into a more symmetrical shape with a significant lowering peak [25]. This can be interpreted that the ADC values became generally higher, presumably by induced necrosis, and the skewness, kurtosis and entropy are lowered by the therapy.

The reported data suggested that ADC histogram parameters may be associated with different histopathological findings in cervical cancer. Previously, only one study investigated direct correlations between histopathology and ADC histogram analysis in cervical cancer [9]. It has been shown that entropy correlated inversely with expression of p53 [9]. However, there were no significant correlations between ADC histogram analysis parameters and tumor cellularity or proliferation

Table 4
Correlations between histopathological features and ADC histogram parameters.

ADC parameters	EGFR	Hif1-alpha	VEGF	Histone 3
Mean, $\times 10^{-3}$ mm^2/s	ρ = **−0.537 (P = 0.022)**	ρ = 0.085 (P = 0.738)	ρ = −0.225 (P = 0.369)	ρ = **−0.555 (P = 0.017)**
Min, $\times 10^{-3}$ mm^2/s	ρ = −0.372 (P = 0.129)	ρ = 0.206 (P = 0.413)	ρ = −0.170 (P = 0.501)	ρ = −0.350 (P = 0.154)
Max, $\times 10^{-3}$ mm^2/s	ρ = −0.313 (P = 0.205)	ρ = 0.129 (P = 0.610)	ρ = −0.032 (P = 0.900)	ρ = −0.176 (P = 0.484)
P10, $\times 10^{-3}$ mm^2/s	ρ = **−0.501 (P = 0.034)**	ρ = 0.204 (P = 0.418)	ρ = −0.219 (P = 0.383)	ρ = **−0.605 (P = 0.008)**
P25, $\times 10^{-3}$ mm^2/s	ρ = **−0.539 (P = 0.021)**	ρ = 0.108 (P = 0.669)	ρ = −0.224 (P = 0.372)	ρ = **−0.610 (P = 0.007)**
P75, $\times 10^{-3}$ mm^2/s	ρ = **−0.562 (P = 0.015)**	ρ = 0.037 (P = 0.883)	ρ = −0.276 (P = 0.267)	ρ = **−0.536 (P = 0.022)**
P90, $\times 10^{-3}$ mm^2/s	ρ = **−0.516 (P = 0.029)**	ρ = 0.027 (P = 0.916)	ρ = −0.310 (P = 0.211)	ρ = **−0.524 (P = 0.026)**
Median, $\times 10^{-3}$ mm^2/s	ρ = **−0.539 (P = 0.021)**	ρ = 0.051 (P = 0.842)	ρ = −0.215 (P = 0.391)	ρ = **−0.554 (P = 0.017)**
Mode, $\times 10^{-3}$ mm^2/s	ρ = **−0.491 (P = 0.039)**	ρ = 0.218 (P = 0.384)	ρ = −0.100 (P = 0.692)	ρ = −0.232 (P = 0.355)
Kurtosis	ρ = −0.030 (P = 0.906)	ρ = 0.207 (P = 0.409)	ρ = −0.340 (P = 0.168)	ρ = −0.315 (P = 0.203)
Skewness	ρ = −0.242 (P = 0.333)	ρ = 0.210 (P = 0.404)	ρ = −0.228 (P = 0.362)	ρ = −0.198 (P = 0.430)
Entropy	ρ = 0.156 (P = 0.536)	ρ = 0.170 (P = 0.499)	ρ = −0.401 (P = 0.09)	ρ = −0.278 (P = 0.265)

Statistically significant correlations are highlighted in bold.

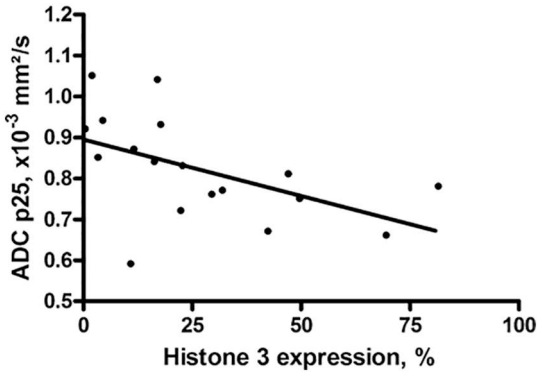

Fig. 3. Correlation graph between ADCp25 and Histone 3 expression. The Spearman correlation coefficient is ρ = −0.610 (P = 0.007).

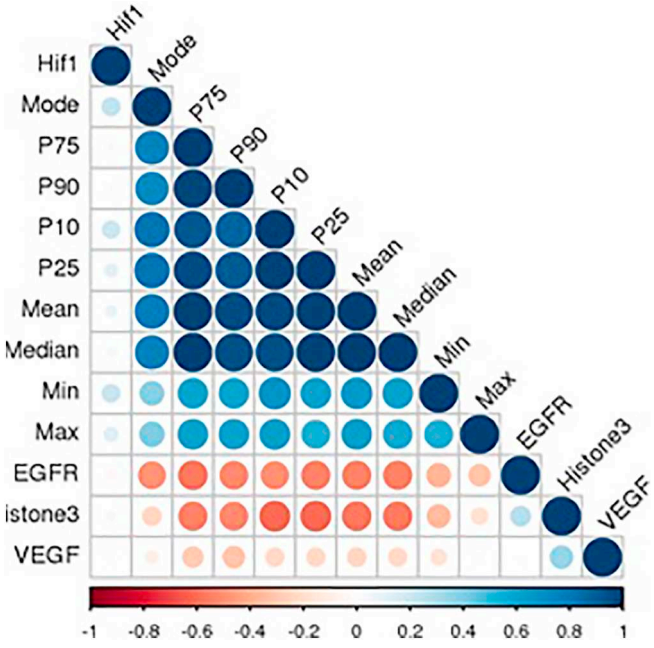

Fig. 4. Spearman's correlation coefficient matrix with color-coded correlation coefficients.

Table 5
The patient sample divided into Her 2- positive and Her 2- negative tumors. There were no statistically significant differences in regard to the Her 2-status.

ADC parameters	Her 2+ (M + SD)	Her 2- (M + SD)	P-value (Mann-Whitney)
Mean, $\times 10^{-3}$ mm^2/s	0.85 + 0.07	0.95 + 0.15	0.11
Min, $\times 10^{-3}$ mm^2/s	0.40 + 0.14	0.55 + 0.26	0.28
Max, $\times 10^{-3}$ mm^2/s	1.56 + 0.21	1.69 + 0.38	0.54
P10, $\times 10^{-3}$ mm^2/s	0.67 + 0.06	0.79 + 0.14	0.07
P25, $\times 10^{-3}$ mm^2/s	0.75 + 0.07	0.86 + 0.13	0.07
P75, $\times 10^{-3}$ mm^2/s	0.93 + 0.08	1.05 + 0.17	0.12
P90, $\times 10^{-3}$ mm^2/s	1.03 + 0.09	1.15 + 0.19	0.20
Median, $\times 10^{-3}$ mm^2/s	0.84 + 0.07	0.94 + 0.13	0.11
Mode, $\times 10^{-3}$ mm^2/s	0.83 + 0.08	0.89 + 0.13	0.22
Kurtosis	4.75 + 2.22	5.74 + 3.34	0.89
Skewness	0.50 + 0.85	0.81 + 0.79	0.45
Entropy	3.68 + 0.87	3.57 + 0.84	0.96

index [9].

In the present study, inverse correlations between ADCmean, mode and several percentiles and EGFR expression were observed. EGFR is an important tyrosine kinase receptor, which is expressed in different type of tumors and leads to cellular proliferation [26]. EGFR expression is associated with various cellular pathways, such as proliferation, angiogenesis, metastasis, apoptosis inhibition, chemoresistance, and radioresistance [17,26]. High EGFR expression might be an independent predictor of poor response to radiotherapy or chemo-radiation, poor disease-free survival and poor overall survival [15]. Therefore, it might be important to predict EGFR expression with imaging modalities without tumor biopsy.

Furthermore, we also analyzed associations between imaging parameters and Her2 expression in cervical cancer. Her2 is also a cell surface protein of the EGFR family with an important role regarding diagnostic and prognosis in several malignancies, especially in breast cancer [27]. According to the literature, only a small portion of cervical cancer, namely 10%, is Her2-positive [28]. Her2-overexpression is also associated with a poor prognosis in cervical cancer [29]. We found no significant differences between tumors according to their Her2-status indicating that the microstructure of cervical cancers might not be altered enough between these entities.

Furthermore, the present study identified moderate inverse correlations between ADC histogram parameters and histone 3 expression. As reported previously, over 90% of cervical cancer show histone 3 expression and it is associated with human papilloma virus infection, a

major cause of cervical cancer [30]. Histones are highly alkaline proteins localized in eukaryotic cell nuclei. Histone package and order the DNA into structural units called nucleosomes [31]. Histone 3 expression was identified to be associated with low grading, low FIGO-classification, low T-status and negative N-status in cervical cancer as well as with a poor prognosis [30]. Presumably, the identified associations between ADC histogram parameters and histone 3 expression might be caused by diffusion restriction due to nucleic sizes [32]. To the best of our knowledge, previously, no study investigated possible associations between histone expression and ADC values.

Additionally, we analyzed associations of ADC histogram based parameters and expression of VEGF. VEGF is a specific mitogen for vascular endothelial cells [16]. In hypoxic state, the expression of VEGF is up-regulated by activated oncogenes and a number of cytokines. VEGF initiates endothelial cell proliferation and angiogenesis, as well as the permeability of tumor blood vessel [16]. As reported previously, VEGF expression was significantly related to disease-free survival and overall survival in patients who received primary radiotherapy or neoadjuvant chemotherapy [15]. The present study could not identify statistically significant correlations between ADC values and VEGF. There may be caused by several reasons. Firstly, according to the literature, only a small portion of DWI is perfusion sensitive, namely low b-values up to 200 s/mm^2 [33]. In the present study, a high b-value 1000 s/mm^2 was used and, therefore, the calculated ADC parameters cannot reflect tumor perfusion. Previously, only one study investigated associations between VEGF expression and microvessel density with ADC in cervical cancer [20]. This study used a special parameter, namely the ADC difference value, including a very high b value (3000 s/mm^2) and a low b value (100 s/mm^2) [20]. This parameter was able to reflect VEGF expression ($r = 0.521$, $P < 0.001$) and microvessel density ($r = 0.940$, $P < 0.001$) [20].

Previously, no study analyzed possible associations between Hif1-alpha expression and ADC values in cervical cancer. According to the literature, Hif1-alpha plays an important role in the adaptive cellular response to hypoxia [34]. It is also well known that Hif1 overexpression is associated with a poor survival in cervical cancer patients [34]. In the present study, no significant associations between expression of Hif1-alpha and ADC histogram analysis parameters were identified. Our results are in agreement with those of Swartz et al., who also did not show significant associations between ADC and expression of Hif1-alpha in head and neck cancer [35]. However, in prostate cancer [36] and rectal cancer [37], moderate positive correlations between ADC histogram parameters and Hif1-alpha expression were reported.

Overall, our study showed that ADC histogram analysis parameters might be able to reflect expression of oncogenic markers in uterine cervical cancer, and cannot be used as surrogate parameters for angiogenesis and/or hypoxia related parameters.

The present study also could show that ADC histogram parameters have a good interreader variability, which is of great importance for possible usage of ADC values as biomarkers in clinical practice. The agreement coefficient only differed slightly between the parameters indicating that everyone might be suitable for clinical practice. This is in good agreement with the literature. In fact, some previous reports also showed a good to excellent interreader agreement of ADC histogram analysis parameters in various tumor entities [10,38].

There are several limitations of the present study. Firstly, a small patient sample was investigated, comprising only of squamous cell carcinomas. Secondly, the histogram analysis was performed as a whole lesion measurement, whereas the histopathology was only performed on biopsy specimens.

In conclusion, histogram analysis of ADC showed a good interreader agreement and, therefore, can be recommended as a robust investigation in cervical cancer. ADC histogram parameters might be associated with the expression of EGFR and histone 3 in cervical squamous cell carcinomas. However, these associations alone might not be strong enough for a reliable prediction in clinical routine. ADC histogram parameters cannot reflect Her 2 status, expression of VEGF and Hif1-alpha in cervical cancer.

Abbreviations

MRI	magnetic resonance imaging
DWI	diffusion weighted imaging
ADC	apparent diffusion coefficient
EGFR	epidermal-growth factor
Hif1-alpha	hypoxia-inducible factor 1-alpha
VEGF	vascular endothelial growth factor
Her 2	human epidermal growth factor receptor 2
ROI	region of interest

Acknowledgements

None.

Funding

This research did not receive any specific grant from funding agencies in the public, commercial, or not-for-profit sectors.

Author's contribution

HJM and PG performed MRI analysis. HJM and AS wrote the manuscript. GH performed statistical analysis. AKH performed histopathology analysis. All authors read and approved the final manuscript.

Ethics approval and consent to participate

The study was approved by the institutional review committee and was in compliance with HIPAA regulations. Due to the retrospective nature of the study, informed consent for retrospective data analysis was waved by the institutional review board.

References

[1] Jemal A, Bray F, Center MM, Ferlay J, Ward E, Forman D. Global cancer statistics. CA Cancer J Clin 2011;61:69–90.
[2] Sala E, Wakely S, Senior E, Lomas D. MRI of malignant neoplasms of the uterine corpus and cervix. AJR Am J Roentgenol 2007;188:1577–87.
[3] Padhani AR, Liu G, Koh DM, Chenevert TL, Thoeny HC, Takahara T, et al. Diffusion-weighted magnetic resonance imaging as a cancer biomarker: consensus and recommendations. Neoplasia 2009;11:102–25.
[4] Surov A, Meyer HJ, Wienke A. Correlation between apparent diffusion coefficient (ADC) and cellularity is different in several tumors: a meta-analysis. Oncotarget 2017;35:59492–9.
[5] Liu Y, Bai R, Sun H, Liu H, Wang D. Diffusion-weighted magnetic resonance imaging of uterine cervical cancer. J Comput Assist Tomogr 2009;33:858–62.
[6] Liu Y, Ye Z, Sun H, Bai R. Clinical application of diffusion-weighted magnetic resonance imaging in uterine cervical cancer. Int J Gynecol Cancer 2015;25:1073–8.
[7] Surov A, Meyer HJ, Schob S, et al. Parameters of simultaneous 18F-FDG-PET/MRI predict tumor stage and several histopathological features in uterine cervical cancer. Oncotarget 2017;8:28285–96.
[8] Just N. Improving tumour heterogeneity MRI assessment with histograms. Br J Cancer 2014;111:2205–13.
[9] Schob S, Meyer HJ, Pazaitis N, et al. ADC histogram analysis of cervical cancer aids detecting lymphatic metastases-a preliminary study. Mol Imaging Biol 2017;19:953–62.
[10] Meng J, Zhu L, Zhu L, et al. Whole-lesion ADC histogram and texture analysis in predicting recurrence of cervical cancer treated with CCRT. Oncotarget 2017;8:92442–53.
[11] Guan Y, Shi H, Chen Y, et al. Whole-lesion histogram analysis of apparent diffusion coefficient for the assessment of cervical cancer. J Comput Assist Tomogr 2016;40:212–7.
[12] Heo SH, Shin SS, Kim JW, et al. Pre-treatment diffusion-weighted MR imaging for predicting tumor recurrence in uterine cervical cancer treated with concurrent chemoradiation: value of histogram analysis of apparent diffusion coefficients. Korean J Radiol 2013;14:616–25.
[13] Downey K, Riches SF, Morgan VA, et al. Relationship between imaging biomarkers of stage I cervical cancer and poor-prognosis histologic features: quantitative histogram analysis of diffusion-weighted MR images. AJR Am J Roentgenol 2013;200:314–20.

[14] Lin Y, Li H, Chen Z, Ni P, Zhong Q, Huang H, et al. Correlation of histogram analysis of apparent diffusion coefficient with uterine cervical pathologic finding. AJR Am J Roentgenol 2015;204:1125–31.
[15] Gadducci A, Guerrieri ME, Greco C. Tissue biomarkers as prognostic variables of cervical cancer. Crit Rev Oncol Hematol 2013;86:104–29.
[16] Iwasaki K, Yabushita H, Ueno T, Wakatsuki A. Role of hypoxia-inducible factor-1α, carbonic anhydrase-IX, glucose transporter-1 and vascular endothelial growth factor associated with lymph node metastasis and recurrence in patients with locally advanced cervical cancer. Oncol Lett 2015;10:1970–8.
[17] Bumrungthai S, Munjal K, Nandekar S, et al. Epidermal growth factor receptor pathway mutation and expression profiles in cervical squamous cell carcinoma: therapeutic implications. J Transl Med 2015;13:244.
[18] Yang W, Qiang JW, Tian HP, Chen B, Wang AJ, Zhao JG. Multi-parametric MRI in cervical cancer: early prediction of response to concurrent chemoradiotherapy in combination with clinical prognostic factors. Eur Radiol 2018;28:437–45.
[19] Xue H, Ren C, Yang J, et al. Histogram analysis of apparent diffusion coefficient for the assessment of local aggressiveness of cervical cancer. Arch Gynecol Obstet 2014;290:341–8.
[20] Liu Y, Ye Z, Sun H, Bai R. Grading of uterine cervical cancer by using the ADC difference value and its correlation with microvascular density and vascular endothelial growth factor. Eur Radiol 2013;23:757–65.
[21] Yang W, Qiang JW, Tian HP, Chen B, Wang AJ, Zhao JG. Minimum apparent diffusion coefficient for predicting lymphovascular invasion in invasive cervical cancer. J Magn Reson Imaging 2017;45:1771–9.
[22] Meng J, Zhu L, Zhu L, et al. Histogram analysis of apparent diffusion coefficient for monitoring early response in patients with advanced cervical cancers undergoing concurrent chemo-radiotherapy. Acta Radiol 2017;58:1400–8.
[23] Thapa D, Wang P, Wu G, Wang X, Sun Q. A histogram analysis of diffusion and perfusion features of cervical cancer based on intravoxel incoherent motion magnetic resonance imaging. Magn Reson Imaging 2018 Jun 25;55:103–11. (pii: S0730-725X(18)30181-4).
[24] Xue H, Ren C, Yang J, et al. Histogram analysis of apparent diffusion coefficient for the assessment of local aggressiveness of cervical cancer. Arch Gynecol Obstet 2014;290:341–8.
[25] Meng J, Zhu L, Zhu L, et al. Apparent diffusion coefficient histogram shape analysis for monitoring early response in patients with advanced cervical cancers undergoing concurrent chemo-radiotherapy. Radiat Oncol 2016;11:141.
[26] Hu YF, Lei X, Zhang HY, et al. Expressions and clinical significance of autophagy-related markers Beclin1, LC3, and EGFR in human cervical squamous cell carcinoma. Onco Targets Ther 2015;8:2243–9.
[27] Slamon D, Eiermann W, Robert N, et al. Adjuvant trastuzumab in HER2-positive breast cancer. N Engl J Med 2011;365:1273–83.
[28] Lesnikova I, Lidang M, Hamilton-Dutoit S, Koch J. HER2/neu (c-erbB-2) gene amplification and protein expression are rare in uterine cervical neoplasia: a tissue microarray study of 814 archival specimens. APMIS 2009;117:737–45.
[29] Fuchs I, Vorsteher N, Bühler H, et al. The prognostic significance of human epidermal growth factor receptor correlations in squamous cell cervical carcinoma. Anticancer Res 2007;27:959–63.
[30] Beyer S, Zhu J, Mayr D, et al. Histone H3 acetyl K9 and histone H3 tri methyl K4 as prognostic markers for patients with cervical cancer. Int J Mol Sci 2017;18:E477.
[31] Bannister AJ, Kouzarides T. Regulation of chromatin by histone modifications. Cell Res 2011;21:381–95.
[32] Xu J, Does MD, Gore JC. Sensitivity of MR diffusion measurements to variations in intracellular structure: effects of nuclear size. Magn Reson Med 2009;61:828–33.
[33] Iima M, Le Bihan D. Clinical intravoxel incoherent motion and diffusion MR imaging: past, present, and future. Radiology 2016;278:13–32.
[34] Huang M, Chen Q, Xiao J, et al. Overexpression of hypoxia-inducible factor-1α is a predictor of poor prognosis in cervical cancer: a clinicopathologic study and a meta-analysis. Int J Gynecol Cancer 2014;24:1054–64.
[35] Swartz JE, Driessen JP, van Kempen PMW, et al. Influence of tumor and microenvironment characteristics on diffusion-weighted imaging in oropharyngeal carcinoma: a pilot study. Oral Oncol 2018;77:9–15.
[36] Ma T, Yang S, Jing H, Cong L, Cao Z, Liu Z, et al. Apparent diffusion coefficients in prostate cancer: correlation with molecular markers Ki-67, HIF-1α and VEGF. NMR Biomed 2018;31:e3884.
[37] Meng X, Li H, Kong L, et al. MRI in rectal cancer: correlations between MRI features and molecular markers Ki-67, HIF-1α, and VEGF. J Magn Reson Imaging 2016;44:594–600.
[38] Nakajo M, Fukukura Y, Hakamada H, et al. Whole-tumor apparent diffusion coefficient (ADC) histogram analysis to differentiate benign peripheral neurogenic tumors from soft tissue sarcomas. J Magn Reson Imaging 2018 Feb 22. https://doi.org/10.1002/jmri.25987.